# INTEGRALS ALONG CENTRAL SLICES THROUGH THE POWER SPECTRUM AND THE AUTO CORRELATION FUNCTION

# H. GLÜNDER

Lehrstuhl für Nachrichtentechnik, Technische Universität München, Arcisstrasse 21, D-8000 Munich 2, Fed. Rep. Germany

Received 5 September 1985

Two features often used in the field of pattern recognition are shown to be mathematically identical: the integral values taken along straight lines through the origin of either the power spectrum or the auto correlation function of a pattern. Furthermore an opto-digital processor is proposed that allows the evaluation of this feature without the need of producing either the Fourier transform or the auto correlation function of the pattern. The theoretically deduced identity is corroborated by results from experiments based on these three methods.

## **1. Introduction**

The worth of the Fourier power spectrum as well as the autocorrelation function for the analysis and recognition of two-dimensional patterns is well recognized [1–8]. Besides their characteristic of indicating pattern periodicities, and of being geometrically centered (in the case of real valued pattern functions) it is mainly their shift invariance that makes them so attractive for pattern analysis purposes. Two integral features are commonly extracted from either of these signal representations in order to reduce their dimensionality and thus to allow easier postprocessing:

(i) Integrals taken along straight lines through the origin as a function of their orientations (angle feature).

(ii) Integrals taken along concentric circles around the origin as a function of their radii (scale feature).

Only one half-plane of either pattern representation must be evaluated if real valued patterns are investigated (point symmetry due to properties of the Fourier transformation). These feature functions show suitable further invariances: The first is size invariant, the second is rotation invariant.

Both feature functions can be evaluated using optical parallel computing techniques. The Fourier spectrum can be generated quite precisely by a co-

0 030-4018/86/\$03.50 © Elsevier Science Publishers B.V. (North-Holland Physics Publishing Division)

herent-optical Fourier transformation if the input patterns are available as transparencies, or if suitable spatial light modulators can be used. The coherentoptical generation of the auto correlation function, however, is more complicated since, in general, a two-step process is necessary. If the requirements concerning the space bandwidth product (SBP) are not too high, typically less than that presented by a TV half-frame image (SBP  $< 10^5$ ), an incoherentoptical ground-glass auto correlator [11] ("shadow casting"-principle [9,10]) can be used. Usually the features are extracted from the light distributions by suitable apertures and photodetectors (e.g., rotating slits or sectors together with light collecting optics and sensors) [2,12,13], or by the well-known and convenient wedge-ring photodetector arrangement [7,14-18].

In this paper the angle feature functions are investigated. It is shown that the constituting line integral values computed from the power spectrum are identical to those taken along orthogonal lines through the autocorrelation function of a pattern. In other words, it is demonstrated that the feature function resulting from spatial integrations over a rotating straight line through the origin of the power spectrum is identical to the (generalized) angle chord function [3,17-20], except for a shift of 90°. A third method for the evaluation of this feature function, which can be realized with an opto-digital processor, is described. Due to its incoherent-optical first stage there are no restrictions concerning the physical representation of the input pattern (transparent, diffuse reflecting, self-luminous, etc.) and there is no need for a coherent light source. Contrary to the ground-glass correlator the SBP of this preprocessor is not limited by diffraction occurring at the input transparency [21]. Since in most cases a digital computer is used for further data processing anyway (e.g., classification) [15-17,22,23] it is no problem to perform some additional arithmetic operations on the electronically sensed output of the optical stage.

#### 2. Mathematical deductions

For simplicity ideal line integrals are considered here instead of more realistic integrals taken over slits of finite extent or sectors. Let the autocorrelation function of a two-dimensional pattern f(x, y) be denoted by a(x, y) and the pattern's power spectrum by  $A(u, v) = \mathcal{F}{a(x, y)}$ . (Note that in this paper capital letters are used for functions in the frequency domain and all integrations extend from  $-\infty$  to  $+\infty$ ; the symbol  $\mathcal{F}{\dots}$  denotes Fourier transformation). Given the autocorrelation function in polar coordinates, then the angle chord function is defined by

$$n(\theta) = \int \tilde{a}(\tilde{r},\theta) \,\mathrm{d}\tilde{r} \tag{1}$$

with  $\tilde{r} = \sqrt{x^2 + y^2}$  and  $\theta = \arctan(y/x)$ , and the corresponding notation of the power spectral angle feature is

$$M(\phi) = \int \tilde{A}(\tilde{p}, \phi) \,\mathrm{d}\tilde{p} \tag{2}$$

with  $\tilde{p} = \sqrt{u^2 + v^2}$  and  $\phi = \arctan(v/u)$ . Obviously these functions show a periodicity of 180°. Using the gating property of  $\delta$ -functions, these features can be written in the following way (fig. 1a)

$$n(\theta) = \iint a(x, y) \cdot \delta(s) \, \mathrm{d}x \, \mathrm{d}y \tag{3}$$

with  $s = -x \sin \theta + y \cos \theta$  and  $r = x \cos \theta + y \sin \theta$ , where the  $\delta$ -line function defines the straight line of integration with an orientation angle  $\theta$ , and (fig. 1b)

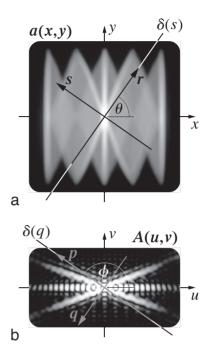


Fig. 1. Extraction of the angle chord function from the autocorrelation function (a) and of the power spectral angle feature from the corresponding power spectrum (b).

$$M(\phi) = \iint A(u, v) \cdot \delta(q) \, \mathrm{d}u \, \mathrm{d}v \tag{4}$$

with  $q = -u \sin \phi + v \cos \phi$  and  $p = u \cos \phi + v \sin \phi$ , i.e. with an integration line having the orientation angle  $\phi$ . Applying the generalized version of Parseval's formula [24]

$$\iint g_1(x, y) \cdot g_2^*(x, y) \, \mathrm{d}x \, \mathrm{d}y$$
  
= 
$$\iint G_1(u, v) \cdot G_2^*(u, v) \, \mathrm{d}u \, \mathrm{d}v$$
 (5)

and substituting  $g_1(x, y)$  by a(x, y) and  $g_2(x, y)$  by the (real valued)  $\delta$ -line function from eq. (3), then, by taking into account the Fourier correspondence of the latter

$$\mathscr{F}\left\{\delta(s)\right\} = \delta(q), \tag{6}$$

and with  $\phi = \theta + 90^{\circ}$ , the equivalence of the two functions is evident

$$n(\theta) = M(\theta + 90^\circ) = M(\phi).$$
<sup>(7)</sup>

Volume 57, number 1

# 3. Approach via projections

A third method for the evaluation of the angle feature is based on the Fourier projection theorem (central slice theorem) [25] which plays an important role, for instance, in the field of tomographic image reconstruction [26,27]. (Gindi and Gmitro [28] propose to synthesize the whole power spectrum from pattern projections from which further features can be extracted.) Fig. 2 illustrates this theorem: The parallel projection  $t_{\theta}(s)$  gained under the angle  $\theta$  from a pattern f(x, y) can be expressed by integrations along lines that are collinear to the projection direction (fig. 2a)

$$t_{\theta}(s) = \int f(x, y) \,\mathrm{d}r \,. \tag{8}$$

Considering the two-dimensional Fourier transformation of f(x, y) with respect to the rotated coordinate system (fig. 2b)

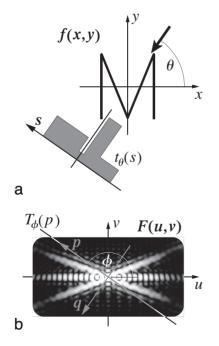


Fig. 2. Explanation of the Fourier projection theorem: Projection  $t_{\theta}(s)$  of pattern f(x, y) (a) and corresponding central slice function  $T_{\phi}(p)$  of the pattern's complex spectrum F(u, v) (b).

$$F(u,v) = \iint f(x,y) \cdot \exp\left[-j \cdot 2\pi(-rq+sp)\right] dr ds, \quad (9)$$

a central slice  $T_{\phi}(p)$  of the complex spectrum F(u, v) can then be written as

$$T_{\phi}(p) = F(u, v)|_{q=0}$$
  
= 
$$\int \left[ \int f(x, y) \, \mathrm{d}r \right] \exp\left[-j \cdot 2\pi sp\right] \mathrm{d}s, \qquad (10)$$

which is the one-dimensional Fourier transform of  $t_{\theta}(s)$ . The basic version of Parseval's formula for one-dimensional functions

$$\int \left| g(x) \right|^2 \mathrm{d}x = \int \left| G(u) \right|^2 \mathrm{d}u \tag{11}$$

is now used to relate the integral energies of the functions in eq. (8) and (10)

$$M(\phi) = \int |T_{\phi}(p)|^2 dp$$
  
=  $\int |t_{\theta}(s)|^2 ds = \int |\int f(x, y) dr|^2 ds$  (12)

with

$$\int |T_{\phi}(p)|^2 \,\mathrm{d}p = \iint A(u,v) \cdot \delta(q) \,\mathrm{d}u \mathrm{d}v \,.$$

For real valued patterns it is sufficient to square the integral values of eq. (8) and thus, beside this, only summations are required for the computation.

With this mathematical vehicle it is again possible to demonstrate the equivalence formulated in eq. (7), since the power spectral angle feature can be written as

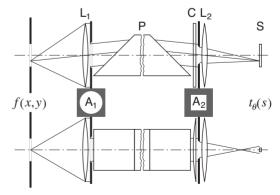


Fig. 3. Incoherent-optical preprocessor for the evaluation of the angle feature function via projections.

Volume 57, number 1

$$M(\phi) = \int \hat{T}_{\phi}(p) \, \mathrm{d}p = \hat{t}_{\theta}(s=0)$$
  
= 
$$\iint a(x, y) \cdot \delta(s) \, \mathrm{d}x \, \mathrm{d}y = n(\theta)$$
 (13)

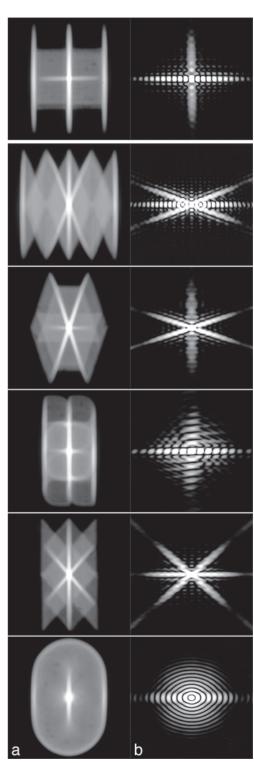
Function  $\hat{T}_{\phi}(p)$  is a central slice through the power spectrum A(u, v) and the projection value  $\hat{t}_{\theta}(0)$  is obtained from the line integral through the origin of the auto correlation function a(x, y) with  $\hat{T}_{\phi}(p) = \mathcal{F}\{\hat{t}_{\theta}(s)\}$ .

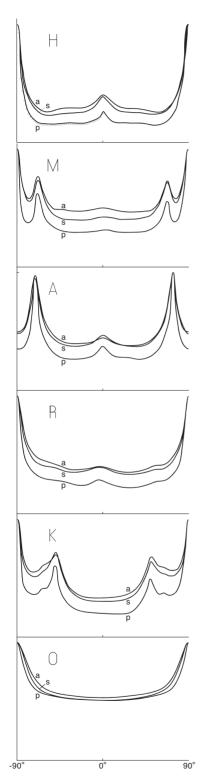
### 4. Experiments

The three methods were applied to line-like input patterns (36 capital letters and numerals). Fig. 4a shows incoherent-optically produced autocorrelation functions of a sample of six characters (shown together with the plots in (fig. 5) that were continuously scanned by a sufficiently narrow slit rotating around the origin. The light intensity behind this slit mask is measured with an integrating sphere and the amplified photo-current is directly recorded by an x,y-writer. The original plots, as a function of the angle  $\theta$ , are shown as curves "a" in fig. 5. A similar measuring technique was applied to the corresponding, coherent-optically computed Fourier spectra which are depicted in fig. 4b. The resulting intensity versus angle  $\phi$  functions in fig. 5 are indicated by the letter "s". Each curve is normalized to its maximum.

The projection based approach (eq. (12)) was realized using an astigmatic imaging system "C", (cylindrical lens correlator) and a CCD-line detector "S" for the opto-electric conversion of the projections. The image rotation is achieved by a stepper-motor driven Dove prism "P" (similar optical elements are feasible). The basic arrangement is sketched in fig. 3. For each angular position the 1024 photo-voltages from the sensor are digitized and read into a  $\mu$ -processor system (Z 80). For every projection, this processor squares each sample value and then, sums them. The results are shown as curves "p" in fig. 5. (The plot gained from the pattern "H" contains, for the first 90°, the angular sampling points separated

Fig. 4. Incoherent-optically computed autocorrelation functions (a) and the corresponding coherent-optically gained power spectra (b) of the letters "H MARKO".





by  $\Delta \theta = 2^{\circ}$ ; all curves "p" are hand-drawn according to the original computer protocol; the curves are normalized as well.)

#### 5. Discussion

It is obvious from the graphs in fig. 5, representing those obtained from the other 30 investigated patterns, that the results from the three computational methods are in good qualitative accordance, i.e., the plots for each pattern have quite similar shape. Even details (cf. the pattern "K") are present in all three curves. The absolute differences between the results are suspected to be due to the following experimental conditions: (1) The slightly different input patterns used for the three approaches (mainly differing in the "line-width to symbol size ratio", due to photographic processes), (2) the finite slit-widths, (3) the finite precision in the adjustment of the rotation centre (which causes severe errors due to the high intensities at the origin), and (4) the moderate SBP of the applied auto correlation technique [21].

The most pronounced curves result from the projection based method. There are no shortcomings as in (2) to (4). The SBP of the proposed processor depends mainly on the size of the apertures and the quality of the optical elements. The system's upper bandlimit, defined by the aperture orthogonal to the refracting axis of the cylindrical lens can easily be chosen to meet the sampling condition associated with a given detector arrangement. The maximal angular sampling increment however, is more difficult to determine. For line-like patterns it can be derived from their line-width.

Some specific advantages and possibilities of the projection based approach are now summarized:

- The incoherent-optical preprocessor works with white or coloured light. Therefore, even diffuse reflecting pattern representations can be accepted and possible colour information is preserved.

- The imaging system permits an easy adaptation of the pattern size or input area to the sensor dimensions.

Fig. 5. Angle feature functions of six letters: Extracted from their autocorrelation functions "a", from their power spectra "s" and via pattern projections "p".

– The speed of the processing depends on the type of sensor, the image rotator and the digital processor. If a fast read out sensor is available together with a fast data acquisition circuit it seems possible to process up to 30 patterns per second (with the prism rotating at about 500 rpm, a  $\Delta\theta$  of some degree and about 10<sup>3</sup> samples per projection).

- Self-luminous patterns, e.g., from a CRT-display, can be processed as well, although care must be taken for a temporal synchronisation between the display and the sensor.

– A CRT-display can also be used to rotate a pattern if the deflection voltages are suitably computed. The speed, however, is limited by the number of frames per second of the display system. In such a system it is possible to generate the projections directly on the display if the linear dynamic range of the screen is high enough.

- The squaring operation and the succeeding integration can also be performed by analog-electronic circuits if the accuracy and stability are sufficient.

## 6. Digital evaluation

An additional investigation concerning the computational effort (defined by the number of multiplications) for a purely digital evaluation of the angle feature, either in the frequency domain, or via projections led to the following insights: Supposing an optimized FFT-algorithm, a bilinear interpolation scheme and an input with  $n \times n$  samples, then the effort is lower for the frequency domain approach if more than *m* integral values are to be calculated, e.g., m = 4, 6, 8 for n = 64, 256, 1024 respectively.

This is due to the many spatial interpolations necessary for the evaluation of the projections. The accuracy of the features however, especially for patterns of large DC-component, is essentially higher for the projection based approach. The reason is that the simple bilinear interpolation yields considerable errors for strongly varying signals as they occur preferably in the spectral domain in the vicinity of the DC-term.

Since the digital computation of a pattern's Fourier transform is quite time consuming, not to speak of its autocorrelation function, the proposed opto-digital method represents a rather fast and easily implemented alternative.

#### 7. Conclusion

Obviously, integrals taken along central slices are not identical to those computed from sector-shaped areas. Nevertheless, it has been shown that features gained, for instance, from wedge samples either of the Fourier power spectrum or of the autocorrelation function of a pattern, are related according to the Parseval formula (eq. (5)). Speaking in more general terms, the similarity between a practical integration area and its Fourier transform determines the similarity between the features that are gained with such an integrating device in either domain. Casasent and Chang wrote: "... the physical significance of the two representations (wedge-ring detector samples of the Fourier transform and the autocorrelation) is quite different. We make no effort to decide which is best for pattern recognition" [17]. The presented considerations allow for the quantification of these differences and can help in choosing the better suited feature for a specific pattern recognition task.

## Acknowledgements

I thank R. Bürger for performing the opto-digital experiments and U. Nehmzow for the digital computations. Thanks to my colleague R. Bamler for very essential advice and to H. Platzer and Prof. H. Marko for their interest and support.

# References

- [1] L.P. Horwitz and G.L. Shelton, Proc. IRE 49 (1961) 175.
- [2] G.G. Lendaris and G.L.Stanley, Proc. IEEE 58 (1970) 198.
- [3] D.J.H. Moore, IEEE Trans. SMC-2 (1972) 97.
- [4] K. Preston, Proc. IEEE 60 (1972) 1216.
- [5] J. Duvernoy and K. Chalasinska-Macukow, Appl. Optics 20 (1981) 136.
- [6] J. Duvernoy, Optics Comm. 48 (1983) 80.
- [7] D. Casasent and D. Fetterly, Proc. SPIE 456 (1984) 105.
- [8] I. Juvells, S. Vallmitjana, S. Bosch and D. Ros, Optics
- Comm. 51 (1984) 398.
- [9] W. Meyer-Eppler, Optik 1 (1946) 465.
- [10] M.A. Monahan, K. Bromley and R.P. Bocker, Proc. IEEE 65 (1977) 121.
- [11] L.S.G. Kovasznay and A. Arman, Rev. Sci. Instrum. 28 (1957) 793.

Volume 57, number 1

- [12] B.J. Thompson, Proc. IEEE 65 (1977) 62.
- [13] H. Glünder and R. Lenz, Proc. SPIE 370 (1983) 43.
- [14] N. Jensen, H. Kasdan, D.C. Mead and J. Thomasson, Proc. Opt. Comp. Conf. Zürich (1974).
- [15] H.L. Kasdan, Proc. SPIE 117 (1977) 67.
- [16] G.E. Lukes, Proc. SPIE 117 (1977) 89.
- [17] D. Casasent, W.-T. Chang, Appl. Optics 22 (1983) 2087.
- [18] D.G. Nichol, Optics Comm. 48 (1983) 242.
- [19] D.J.H. Moore and D.J. Parker, Pattern Recogn. 6 (1974) 149.
- [20] D.G. Nichol, Optics Comm. 43 (1982) 168.

- [21] E.L. Green, Appl. Optics 7 (1968) 1237.
- [22] D.P. Casasent, in: Optical information processing, ed. S.H. Lee (Springer 1981) p. 181.
- [23] T. Minemoto, I. Tsuchimoto and S. Imi, Optics Comm. 51 (1984) 221.
- [24] R. Bamler, personal communication.
- [25] R.N. Bracewell, Aust. J. Phys. 9 (1956) 198.
- [26] H.H. Barrett and W. Swindell, Proc. IEEE 65 (1977) 89.
- [27] G.T. Herman, ed., Image reconstructions from projections (Springer 1979).
- [28] G.R. Gindi and A.F. Gmitro, Opt. Eng. 23 (1984) 499.